Method of calculations for electron transport in multiterminal quantum systems based on real-space lattice models

H. Q. Xu*
Solid State Physics, Lund University, Box 118, S-221 00 Lund, Sweden
and Physics Department, Dalian University of Technology, Dalian 116024, China
(Received 15 November 2001; published 1 October 2002)

A formalism for the calculations of electron transport in multiterminal quantum systems is presented. The systems are described by tight-binding Hamiltonians. It is shown that by exploiting real-space Green's functions, a problem of the electron transport in a multiterminal system can be reformulated into a problem of the electron transport in an effective two-terminal system and can then be treated using a standard two-terminal method. Applications of the formalism to a three-terminal system, containing a quantum-confined, T-shaped structure, and a four-terminal system, containing a quantum-confined, cross-bar structure, are also presented. It is found that the transmission and reflection probabilities of the two multiterminal quantum systems show complex spectra. The results are explained in terms of the localization properties of the confined states in the systems.

DOI: 10.1103/PhysRevB.66.165305 PACS number(s): 73.63.Nm, 73.21.La, 73.40.Gk, 73.63.Kv

I. INTRODUCTION

The Landauer-Büttiker formulas[1–4] play an essential role in the study of electric properties of small systems where the size of structures is small, compared to the coherence length. For two-terminal electronic devices, it has been shown[1–3,5] that the conductance of the devices, under the assumption of spin degeneracy, can be expressed as $G=(2e^2/h)\mathcal{T}$, where e is the electron charge, h the Planck's constant, and $\mathcal{T}$ the transmission probability of the devices. Various methods have been developed for numerical calculations of the transmission probability $\mathcal{T}$, which include, e.g., mode-matching methods[6–16] and recursive Green's function technique.[17–22]

The electric properties of a multiterminal system can be analyzed in terms of various transmission probabilities between terminals using the Büttiker formula.[4,23] Due to the structure complexity in comparison with a two-terminal system, the calculations for the transmission probabilities have mainly been carried out for relatively simple multiterminal systems.[24–33] As an example, Büttiker *et al.*[24] derived a scattering matrix for a three-terminal junction consisting of homogeneous wires, using a unitary condition and the assumption that the scattering matrix is real. This scattering matrix has an advantage that it can describe various three-terminal junctions by changing a single coupling parameter, and it has been widely used.[34–37] A disadvantage of this formulation is that the scattering matrix is energy independent and the coupling parameter has to be determined from phenomenological arguments. Itoh[32] derived an energy-dependent scattering matrix for three-terminal junctions, and showed that his scattering matrix is an energy-dependent extension of the phenomenological scattering matrix introduced by Büttiker *et al*. However, the formulation is again made only for junctions built from homogeneous wires.

In this paper, we present a general method to calculate various transmission and reflection coefficients and the local density of states for multiterminal systems based on tight-binding models with fluctuating on-site energies in the scattering region. The method treats the energy-dependent scattering matrix at multiterminal junctions exactly. We will show that in general a problem of electron transport in a multiterminal system can be reformulated into a problem of the electron transport in an effective two-terminal system, and can then be treated using a two-terminal method. Although in this work the formulation will be presented only for three- and four-terminal systems, it can easily be generalized to any other multiterminal system. The formulation can be applied to systems which contain, e.g., disorder and/or quantum confinement, such as quantum dots defined by surrounding tunneling junctions. Disorder and quantum confinement have mostly been disregarded in previous calculations for multiterminal systems. The formulation can also be generalized to include electron-electron interaction in much a similar way as we did in Ref. 38.

Examples of the calculations based on the present formulation will also be given. These examples not only serve as a demonstration of the method, but they are also interesting from a physics point of view, in particular, those calculations in which multiterminal quantum-confined systems are treated. It will be shown that the transmission and reflection coefficients of multiterminal quantum-dot systems exhibit complex structures. It will also be shown that these complex spectra can well be interpreted in terms of the local density of states of the systems, calculated within the same frame work of the tight-binding models by a real-space Green's function method (i.e., the Lanczos-Haydock recursion method).[39,40] Furthermore, it will be shown that the transmission and reflection spectra of the multi-terminal systems depend strongly on the position where other leads are attached to an otherwise two-terminal system. This significant result means that by sweeping contact position of a lead, one can in principle map out the wavefunction of quantum states in confined structure by measuring transmissions.

II. FORMALISM AND APPLICATIONS

In this section, a formulation for the calculation of transmission and reflection probabilities of multiterminal systems

will be presented. Tight-binding models are exploited in the formulation. Without a loss of generality, the formulation in this work will only be carried out for systems with a single channel in each of the leads. This is because, using the concept of eigenchannels, it has been shown that a multiple-channel scattering problem can be decomposed into a set of uncoupled single-channel problems.[41,42] In addition, single-channel lead models have been widely and successfully used in the study of various two-terminal systems (for some recent examples, see Refs. 38 and 42–47).

We will begin in Sec. II A with an outline of the method of calculation for two-terminal systems based on a transfer-matrix scheme. In principle, this formulation is quite elementary, but we prefer to present it briefly here because we believe it to be useful to general readers. In Secs. II B and II C, we will show how a problem of the electron transport in multiterminal systems can be treated by converting it into an effective two-terminal problem. In these two subsections we will give the formulation only for three- and four-terminal systems, but the generalization to other multiterminal systems will be straightforward. We will also present examples of calculations after the formulation in each subsection.

A. Two-terminal system

As for calculation, we represent the system in a tight-binding picture. The two ideal wires are placed horizontally on the left- and right-hand sides of an inhomogeneous system. These two ideal leads span lattice sites $-\infty, \ldots, -(N_L+2), -(N_L+1)$ and sites $N_R+1, N_R+2, \ldots, \infty$, respectively. The inhomogeneous system spans lattice sites $-N_L, \ldots, -1, 0, 1, 2, \ldots, N_R-1, N_R$. The Hamiltonian of the system is given by

$$\begin{aligned} H=&\sum_{n=-N_L}^{N_R} \varepsilon_n \; a_n^\dagger a_n \; - \sum_{n=-N_L}^{N_R-1} t(a_{n+1}^\dagger a_n + \text{H.c.}) \\ &+ \sum_{n\leqslant -(N_L+1)} \varepsilon_L \; a_n^\dagger a_n - \sum_{n\leqslant -(N_L+2)} t(a_{n+1}^\dagger a_n + \text{H.c.}) \\ &+ \sum_{n\geqslant N_R+1} \varepsilon_R \; a_n^\dagger a_n - \sum_{n\geqslant N_R+1} t(a_{n+1}^\dagger a_n + \text{H.c.}) \\ &- v_L(a_{-N_L-1}^\dagger a_{-N_L} + \text{H.c.}) - v_R(a_{N_R}^\dagger a_{N_R+1} + \text{H.c.}). \end{aligned} \tag{1}$$

In the above equation, ε_n, with $-N_L \leqslant n \leqslant N_R$, are the on-site energies in the inhomogeneous region, ε_L and ε_R are the on-site energies in the left- and the right-hand-side leads, respectively, and t is the hopping integral which can be related to the lattice constant a and the electron effective mass m^* via $t=\hbar^2/2m^*a^2$.[48] One can then write $\varepsilon_n=\varepsilon_L=U_0+2t$ for $n\leqslant -N_L-1$, $\varepsilon_n=\varepsilon_R=U_0+2t$ for $n\geqslant N_R+1$, and $\varepsilon_n=U_0+U_n+2t$ for $-N_L\leqslant n\leqslant N_R$, where U_0 is the local potential and U_n is the shift of the potential in the inhomogeneous region due to, e.g., impurities, a gate voltage applied, or electron-electron interaction. In the present lattice model, the energy dispersion relation in the ideal leads reads $E(k)=U_0+2t[1-\cos(ka)]$, while the electron velocity v in the leads can be found from $\hbar v=\partial E/\partial k=2at\sin(ka)$.[48] In this work, we shall take a as the unit of length, t as the unit of energy, and $U_0=0$.

The eigensolutions of the Hamiltonian can be obtained by solving

$$H\psi^\dagger = E\psi^\dagger, \tag{2}$$

where

$$\psi^\dagger = \sum_{n=-\infty}^{\infty} c_n a_n^\dagger. \tag{3}$$

It is elementary to show that the expansion coefficients, $\{c_n\}$, in Eq. (3) satisfy the equation

$$(E-\varepsilon_n)c_n + t_{n-1}c_{n-1} + t_n c_{n+1} = 0, \tag{4}$$

where $t_n=\langle n+1|H|n\rangle = t$, except for $n=N_R$ and $-N_L-1$, for which $t_n=v_R$ and v_L, respectively. The above equation can be written as a matrix equation,

$$\begin{bmatrix} c_{n+1} \\ c_n \end{bmatrix} = \mathbf{M}(n,E) \begin{bmatrix} c_n \\ c_{n-1} \end{bmatrix}, \tag{5}$$

where the matrix $\mathbf{M}(n,E)$, defined by

$$\mathbf{M}(n,E) = \begin{bmatrix} -\dfrac{E-\varepsilon_n}{t_n} & -\dfrac{t_{n-1}}{t_n} \\ 1 & 0 \end{bmatrix}, \tag{6}$$

is the transfer matrix, which links the expansion coefficient vector $(c_{n+1},c_n)^T$ to the expansion coefficient vector $(c_n,c_{n-1})^T$.

In a single ideal lead, the eigenfunctions are of the forms $\{\exp(\pm ikna)\}$, where the terms with a positive (negative) sign represent the right- (left-) going waves. In terms of these eigenfunctions, the solutions of the presently studied system in the two lead regions can be written as

$$c_n = \begin{cases} A^L e^{ik^L na} + B^L e^{-ik^L na}, & -\infty < n \leqslant -(N_L+1) \\ A^R e^{ik^R na} + B^R e^{-ik^R na}, & N_R+1 \leqslant n < \infty. \end{cases} \tag{7}$$

It can be shown that the coefficients A^R and B^R are related to the coefficients A^L and B^L via the equation[49]

$$\begin{bmatrix} A^R \\ B^R \end{bmatrix} = \mathbf{T}(E) \begin{bmatrix} A^L \\ B^L \end{bmatrix}, \tag{8}$$

where the transfer matrix $\mathbf{T}(E)$ is given by

$$\mathbf{T}(E)=\begin{bmatrix} e^{-ik^R(N_R+1)a} & 0 \\ 0 & e^{ik^R(N_R+1)a} \end{bmatrix} \times \begin{bmatrix} e^{ik^Ra} & e^{-ik^Ra} \\ 1 & 1 \end{bmatrix}^{-1} \prod_{n=N_R+1}^{-(N_L+1)} \mathbf{M}(n,E) \times \begin{bmatrix} 1 & 1 \\ e^{-ik^La} & e^{ik^La} \end{bmatrix} \begin{bmatrix} e^{-ik^L(N_L+1)a} & 0 \\ 0 & e^{ik^L(N_L+1)a} \end{bmatrix}. \tag{9}$$

In the calculations, it is convenient to introduce a scattering matrix $\mathbf{S}(E)$, and to rewrite Eq. (8) as

$$\begin{bmatrix} A^R \\ B^L \end{bmatrix} = \mathbf{S}(E) \begin{bmatrix} A^L \\ B^R \end{bmatrix}. \tag{10}$$

It is straightforward to show that the scattering matrix $\mathbf{S}(E)$ is related to the transfer matrix $\mathbf{T}(E)$ via

$$\mathbf{S}_{11}(E)=\mathbf{T}_{11}(E)-\mathbf{T}_{12}(E)\mathbf{T}_{22}^{-1}(E)\mathbf{T}_{21}(E),$$

$$\mathbf{S}_{12}(E)=\mathbf{T}_{12}(E)\mathbf{T}_{22}^{-1}(E),$$

$$\mathbf{S}_{21}(E)=-\mathbf{T}_{22}^{-1}(E)\mathbf{T}_{21}(E),$$

$$\mathbf{S}_{22}(E)=\mathbf{T}_{22}^{-1}(E). \tag{11}$$

A unique solution of Eq. (2) can only be obtained after we impose a boundary condition on the electron state $\psi^\dagger$ of the system. Here we are interested in such states that may carry the electric current through the inhomogeneous region from the left to the right. Thus the boundary condition, which is imposed on the state $\psi^\dagger$, is

$$A^L=1 \text{ and } B^R=0. \tag{12}$$

Inserting this boundary condition into Eq. (10), we immediately obtain

$$A^R=\mathbf{S}_{11}(E),$$

$$B^L=\mathbf{S}_{21}(E). \tag{13}$$

The reflectance $\mathcal{R}$ and the transmission probability $\mathcal{T}$ are then obtained from

$$\mathcal{R}=|B^L|^2,$$

$$\mathcal{T}=(v^R/v^L)|A^R|^2=1-\mathcal{R}, \tag{14}$$

where v^R and v^L are the electron velocity in the left- and right-hand-side leads, respectively. In the next two subsections, we shall present the procedures of generalization of the above formalism to multiterminal systems. Here, in the following, we show examples of calculations for two-terminal systems based on the present formalism.

Figure 2 shows the calculations for the transmission and reflection probabilities of symmetric and asymmetric double-barrier structures. In each structure, the confined part is modeled by a piece of wire spanning ten lattice sites, as for the case of $N_L=5$ and $N_R=4$ in the schematic shown in Fig. 1(a). In the calculations, the on-site energies at all the lattice sites ε_L, ε_R and ε_n, with $n=-N_L,-N_L+1,\ldots,N_R-1,N_R$, are assumed to have a value of $2t$. The parameters of the couplings between the confined part and the two semi-infinite leads are assumed to be $v_L=v_R=0.5t$ in the symmetric structure, while in the asymmetric structure the parameters of the couplings are assumed to be $v_L=0.75t$ and $v_R=0.5t$. Figures 2(a) and 2(b) show the results of the calculation for the symmetric system, while Figs. 2(c) and 2(d) show the results for the asymmetric system. It is seen that the transmission probability of the symmetric system exhibits ten resonant peaks with the height of the unit. As a consequence, the reflection probability of the system exhibits ten dips with zero reflections occurring at the same energy posi-

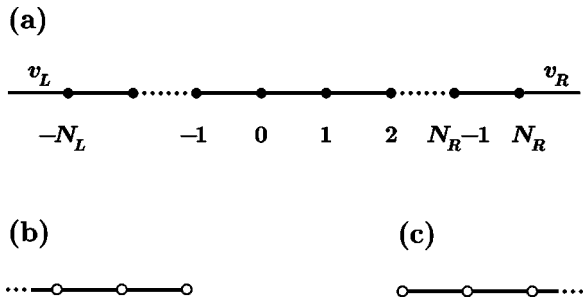

FIG. 1. Lattice model for the two-terminal, quantum-confined system: (a) the confined portion of the system with couplings to two semi-infinite leads described by parameters v_L and v_R, and (b) and (c) the two leads.

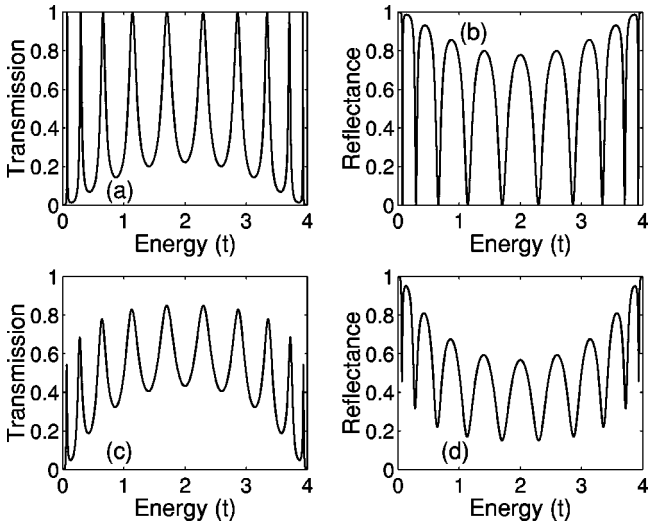

FIG. 2. Transmission and reflection probabilities of the two-terminal, quantum-confined system as shown in Fig. 1, calculated as a function of the electron energy. The confined part in each structure is modeled by a wire spanning ten lattice sites. (a) and (b) show the results of calculation for the symmetric system with the parameters of the couplings, between the confined part and the leads, being assumed to be $v_L=0.5t$ and $v_R=0.5t$. (c) and (d) show the results of the calculation for the asymmetric system with the parameters of the couplings being assumed to be $v_L=0.75t$ and $v_R=0.5t$. All the on-site energies are assumed in the calculations to have a value of $2t$.

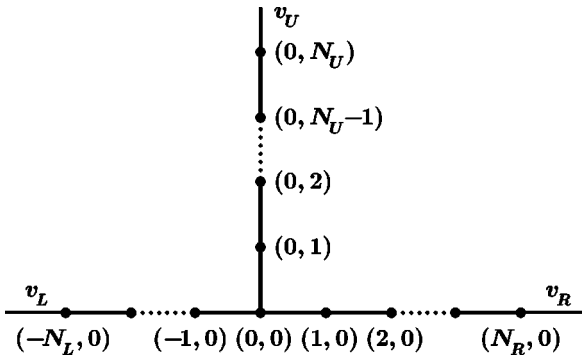

FIG. 3. Lattice model for the three-terminal, quantum-confined system. Here only the confined portion of the system with couplings to three leads described by parameters v_L, v_R, and v_U is given. The three leads are defined similarly as in Fig. 1.

tions as the transmission peaks. These results are consistent with the fact the confined part in the system is modeled by ten lattice sites, and thus the system has ten resonant states localized in between the two tunneling junctions. The ten transmission peaks and the ten corresponding reflection dips are also seen in the calculation for the asymmetric structure [see Figs. 2(c) and 2(d)]. However, all the transmission peaks are lowered in their peak values and the reflection dips become shallower, when compared with the result shown in Fig. 2(a), as expected for the asymmetric double-barrier system. It is also seen in Figs. 2(c) and 2(d) that the transmission peaks and the reflection dips are broadened in their widths. This is due to the fact that the tunneling parameter of v_L has been increased from $0.5t$ to $0.75t$ in the asymmetric structure, and thus the resonant states becomes less localized in the region between the two tunneling junctions.

B. Three-terminal system

Now we present the formulation for the calculation of electron transport in three-terminal systems. Let us consider a three-terminal system constructed by attaching three perfect leads to a T-shaped inhomogeneous region as shown in Fig. 3. In the following, we will label the left-hand-side lead as lead 1, the right-hand-side lead as lead 2, and the middle vertical upper-side lead as lead 3. The couplings of the inhomogeneous region to the left-hand-side and right-hand-side leads are again given by v_L and v_R, while the couplings of the inhomogeneous region to the vertical upper-side lead are given by v_U. Since here the system is modeled by a lattice that extends into two dimensions, it is natural for us to use a double-integer (i,j) scheme to label the lattice sites of the system. In this work, we assign index (0,0) to the cross site. The inhomogeneous region spans horizontal lattice sites $(-N_L,0)$, $(-N_L+1,0)$, $\ldots$,$(N_R-1,0$, $(N_R,0)$ and vertical lattice sites (0,1), (0,2), $\ldots$,$(0,N_U)$, while the three perfect leads span sites $(n,0)$ with $n \leqslant -(N_L+1)$, sites $(n,0)$ with $n \geqslant N_R+1$, and sites $(0,n)$ with $n \geqslant N_U+1$, respectively. The Hamiltonian of the system can be written in a form similar to that in Eq. (1). However, the terms that describe the vertical inhomogeneous region and the middle vertical lead as well as the coupling between them have to be included. To be precise, we write the Hamiltonian of the three-terminal system as

$$
\begin{aligned}
H=&\sum_{n=-N_L}^{N_R} \varepsilon_{n,0}\, a_{n,0}^{\dagger} a_{n,0} - \sum_{n=-N_L}^{N_R-1} t(a_{n+1,0}^{\dagger} a_{n,0} + \text{H.c.}) \\
&+ \sum_{n=1}^{N_U} \varepsilon_{0,n}\, a_{0,n}^{\dagger} a_{0,n} - \sum_{n=0}^{N_U-1} t(a_{0,n+1}^{\dagger} a_{0,n} + \text{H.c.}) \\
&+ \sum_{n\leqslant -(N_L+1)} \varepsilon_L\, a_{n,0}^{\dagger} a_{n,0} - \sum_{n\leqslant -(N_L+2)} t(a_{n+1,0}^{\dagger} a_{n,0} + \text{H.c.}) \\
&+ \sum_{n\geqslant N_R+1} \varepsilon_R\, a_{n,0}^{\dagger} a_{n,0} - \sum_{n\geqslant N_R+1} t(a_{n+1,0}^{\dagger} a_{n,0} + \text{H.c.}) \\
&+ \sum_{n\geqslant N_U+1} \varepsilon_U\, a_{0,n}^{\dagger} a_{0,n} - \sum_{n\geqslant N_U+1} t(a_{0,n+1}^{\dagger} a_{0,n} + \text{H.c.}) \\
&- v_L(a_{-N_L-1,0}^{\dagger} a_{-N_L,0} + \text{H.c.}) - v_R(a_{N_R,0}^{\dagger} a_{N_R+1,0} + \text{H.c.}) \\
&- v_U(a_{0,N_U}^{\dagger} a_{0,N_U+1} + \text{H.c.}). \qquad (15)
\end{aligned}
$$

The scattering properties of the inhomogeneous system are described by the transmission probabilities $\mathcal{T}_{ij}$, defined as the probabilities for electrons incident in lead j to be transmitted into lead i, and the reflection probabilities $\mathcal{R}_{ii}$, defined as the probabilities for incident electrons from lead i to be reflected back into lead i. Let us first consider the calculations for the transmissions $\mathcal{T}_{ij}$. It is important to notice that although each transmission is related to the process of electron transport passing only through two leads, the probability for this process to take place is influenced by the presence of coupling of the system to the third lead. Here we present a formulation for an exact treatment of the problem based on the Hamiltonian given in Eq. (15).

To illustrate the formulation clearly, we take the calculation for the transmission $\mathcal{T}_{21}$ as an example. Recall that $\mathcal{T}_{21}$ is defined as the probability for electrons incident from lead 1 (i.e., the left-hand-side lead) to be transmitted into lead 2 (i.e., the right-hand-side lead). Let us first consider the case of $N_U=0$. In this case a vertical perfect lead is coupled to the site (0,0) of a horizontal inhomogeneous wire. As we did in the formulation for a two-terminal system, we expand the eigensolutions of the three-terminal system as

$$\psi^{\dagger} = \sum_{n=-\infty}^{\infty} c_{n,0} a_{n,0}^{\dagger} + \sum_{n=1}^{\infty} c_{0,n} a_{0,n}^{\dagger}. \qquad (16)$$

Inserting this equation into the Schrödinger equation of the system [Eq. (15)] gives

$$
\begin{aligned}
&(E-\varepsilon_{-1,0})c_{-1,0} + tc_{-2,0} + tc_{0,0} = 0, \\
&(E-\varepsilon_{1,0})c_{1,0} + tc_{0,0} + tc_{2,0} = 0, \\
&(E-\varepsilon_{0,0})c_{0,0} + v_U c_{0,1} + tc_{-1,0} + tc_{1,0} = 0, \\
&v_U c_{0,0} + (E-\varepsilon_{0,1})c_{0,1} + tc_{0,2} = 0, \\
&tc_{0,1} + (E-\varepsilon_{0,2})c_{0,2} + tc_{0,3} = 0, \\
&\cdots\cdots\cdots\cdots. \qquad (17)
\end{aligned}
$$

Similarly as for the left-hand-side and right-hand-side perfect leads [cf. Eq. (7)], the solution in the middle vertical lead (i.e., lead 3) can be written as

$$c_{0,n}=A^U e^{ik^U na}+B^U e^{-ik^U na}, \quad N_U+1\leqslant n<\infty. \quad (18)$$

Note that we have written Eq. (18) in its very general form. However, here we will continue to consider the case of $N_U=0$. In the calculation for the transmission $\mathcal{T}_{21}$, the boundary condition imposed on the solution in lead 3 is $B^U=0$. Using this boundary condition, we can eliminate all the coefficients, $\{c_{0,n}\}$, in Eq. (17) and are able to write

$$\begin{aligned}
&(E-\varepsilon_{-1,0})c_{-1,0}+tc_{-2,0}+tc_{0,0}=0,\\
&(E-\varepsilon_{1,0})c_{1,0}+tc_{0,0}+tc_{2,0}=0,\\
&[E-(\varepsilon_{0,0}+\varepsilon^U_{0,0})]c_{0,0}+tc_{-1,0}+tc_{1,0}=0,\\
&\cdots\cdots\cdots\cdots,
\end{aligned} \quad (19)$$

where $\varepsilon^U_{0,0}=\Sigma^U(E)$ in the case of $N_U=0$, and

$$\Sigma^U(E)=v_U^2 G^U(E) \quad (20)$$

is the self-energy due to the coupling of the horizontal inhomogeneous wire to the semi-infinite perfect lead 3, and $G^U(E)$, which satisfies

$$G^U(E)=[E-\varepsilon_U-t^2G^U(E)]^{-1}, \quad (21)$$

is the Green's function at the first site [i.e., site (0,1) in the present case] of the lead. By solving for the Green's function $G^U(E)$ from the recursive expression of Eq. (21), one obtains

$$G^U(E)=\frac{1}{2t^2}\{(E-\varepsilon_U)-i[4t^2-(E-\varepsilon_U)^2]^{1/2}\}. \quad (22)$$

It is worth pointing out that using the energy dispersion relation of the lead, the Green's function $G^U(E)$ can also be written as $G^U(E)=-t^{-1}\exp(ik^U a)$.

It is seen from Eq. (19) that the calculation for the transmission, $\mathcal{T}_{21}$, of the three-terminal system has now been successfully converted to a calculation for the transmission of an effective two-terminal system. It is also seen that the effect of the coupling of the horizontal inhomogeneous wire to the semi-infinite perfect lead 3 has now been included in the effective on-site energy $\varepsilon_{0,0}+\varepsilon^U_{0,0}$ through the self-energy $\Sigma^U(E)$.

The above results [i.e., Eqs. (19), (20), and (21)] have been derived for the case of $N_U=0$. It can be shown that these results can be generalized to the case of $N_U\neq 0$. Since this derivation follows a rather similar procedure as for the case of $N_U=0$, here we only write down the results. In the case of $N_U\geqslant 1$, the same equation system as shown in Eq. (19) has been obtained after eliminating all the expansion coefficients, $\{c_{0,n}\}$. However, instead of Eq. (20), $\varepsilon^U_{0,0}$ in the effective on-site energy, $\varepsilon_{0,0}+\varepsilon^U_{0,0}$, is now given by

$$\varepsilon^U_{0,0}=\cfrac{t^2}{E-\varepsilon_{0,1}-\cfrac{t^2}{E-\varepsilon_{0,2}-\cfrac{t^2}{\ddots\cfrac{t^2}{E-\varepsilon_{0,N_U}-\Sigma^U(E)}}}}, \quad (23)$$

where the self-energy $\Sigma^U(E)=v_U^2G^U(E)$ and the Green's function $G^U(E)$ are defined exactly in the same way as in the case of $N_U=0$, i.e., by Eqs. (20) and (21), respectively.

As we mentioned before, the equation system shown in Eq. (19) does not contain any of the expansion coefficients, $\{c_{0,n}\}$, associated with the lattice sites in the vertical portion of the three-terminal system. Thus the formula derived in Sec. II A for the transmission of a two-terminal system can be immediately applied to the calculation of the transmission $\mathcal{T}_{21}$ based on the effective two-terminal equation system [i.e., Eq. (19)]. The procedure is briefly outlined as follows. We rewrite Eq. (19) as

$$\begin{bmatrix} c_{n+1,0} \\ c_{n,0} \end{bmatrix}=\tilde{\boldsymbol{M}}(n,E)\begin{bmatrix} c_{n,0} \\ c_{n-1,0} \end{bmatrix}, \quad (24)$$

where the transfer matrix, $\tilde{\boldsymbol{M}}(n,E)$, is now given by

$$\tilde{\boldsymbol{M}}(n,E)=\begin{bmatrix} -\dfrac{E-\tilde{E}_n}{t_n} & -\dfrac{t_{n-1}}{t_n} \\ 1 & 0 \end{bmatrix}. \quad (25)$$

In the above equation, $\tilde{E}_0=\varepsilon_{0,0}+\varepsilon^U_{0,0}$ [recall that $\varepsilon^U_{0,0}$ is given by $\varepsilon^U_{0,0}=\Sigma^U(E)$, i.e., Eq. (20), for $N_U=0$, and by Eq. (23) for $N_U\geqslant 1$], and $\tilde{E}_n=\varepsilon_{n,0}$ for $n\neq 0$. t_n is defined in the same way as in Eq. (6), i.e., $t_n=t$, except for $n=N_R$ and $-N_L-1$, for which $t_n=v_R$ and v_L, respectively. The transfer matrix, $\mathbf{T}(E)$, is obtained by replacing all the matrices $\mathbf{M}(n,E)$ in Eq. (9) with $\tilde{\boldsymbol{M}}(n,E)$. Finally, the transmission $\mathcal{T}_{21}$ is calculated from

$$\mathcal{T}_{21}=(v^R/v^L)|\mathbf{S}_{11}(E)|^2, \quad (26)$$

where the scattering matrix $\mathbf{S}(E)$ is defined in the same way as in Eq. (10) and can simply be calculated from the matrix $\mathbf{T}(E)$ using the relation given in Eq. (11).

A very similar formulation can be made for the transmission, $\mathcal{T}_{31}$, which is defined as the probability for incident electrons from lead 1 (i.e., the left-hand-side lead) to be transmitted to lead 3 (the middle vertical lead). The changes that need to be made in an actual calculation are as follows. First, $\tilde{E}_0=\varepsilon_{0,0}+\varepsilon^U_{0,0}(E)$ in the matrix $\tilde{\boldsymbol{M}}(0,E)$ needs to be replaced by $\tilde{E}_0=\varepsilon_{0,0}+\varepsilon^R_{0,0}(E)$ with

$$\varepsilon_{0,0}^{R}=\cfrac{t^2}{E-\varepsilon_{1,0}-\cfrac{t^2}{E-\varepsilon_{2,0}-\cfrac{t^2}{\ddots\cfrac{t^2}{E-\varepsilon_{N_R,0}-\Sigma^R(E)}}}}, \tag{27}$$

where

$$\Sigma^R(E)=v_R^2 G^R(E) \tag{28}$$

is the self-energy due to the presence of the right-hand-side lead, and

$$G^R(E)=[E-\varepsilon_R-t^2 G^R(E)]^{-1} \tag{29}$$

is the Green's function at the first site [i.e., site $(N_R+1,0)$] of the right-hand-side lead. Second, $\tilde{E}_n=\varepsilon_{n,0}$ in the matrix $\tilde{\boldsymbol{M}}(n,E)$ needs to be replaced by $\tilde{E}_n=\varepsilon_{0,n}$ for all $n>0$. Third, recalculate the transfer matrix $\mathbf{T}(E)$, after all these replacements are made, and the scattering matrix $\mathbf{S}(E)$ from Eq. (11). Finally, calculate the transmission $\mathcal{T}_{31}$ from

$$\mathcal{T}_{31}=(v^U/v^L)|\mathbf{S}_{11}(E)|^2, \tag{30}$$

where v^U is the electron velocity in the upper-side lead.

We shall now present the formulation for the calculation of the reflectance $\mathcal{R}_{11}$ of the three-terminal system. Here, three different, but equivalent, ways of formulation of the problem are described. In the first two ways, the calculation for $\mathcal{R}_{11}$ is carried out at the same time when the calculation for the transmission $\mathcal{T}_{21}$ or $\mathcal{T}_{31}$ is performed. This follows a procedure which is rather similar to the calculation of the reflectance $\mathcal{R}$ for a two-terminal system. For example, in the case when the transmission $\mathcal{T}_{21}$ is calculated, after replacing all matrices $\boldsymbol{M}(n,E)$ in Eq. (9) by the matrices $\tilde{\boldsymbol{M}}(n,E)$ given by Eq. (25), we calculate both the submatrices $\mathbf{S}_{11}$ and $\mathbf{S}_{21}$ using Eq. (11). The transmission probability $\mathcal{T}_{21}$ is related to the submatrix $\mathbf{S}_{11}$ via Eq. (26), while the reflectance $\mathcal{R}_{11}$ is given by

$$\mathcal{R}_{11}=|\mathbf{S}_{21}(E)|^2. \tag{31}$$

In the case when $\mathcal{T}_{31}$ is calculated, the same procedure is implemented, except that $\tilde{E}_0=\varepsilon_{0,0}+\varepsilon_{0,0}^U$ needs to be replaced by $\tilde{E}_0=\varepsilon_{0,0}+\varepsilon_{0,0}^R$ and $\tilde{E}_n=\varepsilon_{n,0}$ needs to be replaced by $\tilde{E}_n=\varepsilon_{0,n}$ for all $n\geqslant 1$.

A third way of the calculation of the reflectance $\mathcal{R}_{11}$ exploits a very different procedure. In this third way, the reflectance $\mathcal{R}_{11}$ can be calculated directly from a simple formula, which is to be derived below, with no need for computing the scattering matrix $\mathbf{S}(E)$. The derivation of the formula may start from Eq. (19). By eliminating all the coefficients, $c_{n,0}$, with $n\geqslant 1$ in this equation, one obtains

$$(E-\tilde{\varepsilon}_{0,0})c_{0,0}+tc_{-1,0}=0,$$

$$(E-\varepsilon_{-1,0})c_{-1,0}+tc_{-2,0}+tc_{0,0}=0,$$

$$(E-\varepsilon_{-2,0})c_{-2,0}+tc_{-3,0}+tc_{-1,0}=0,$$

$$\cdots\cdots\cdots\cdots, \tag{32}$$

where the effective on-site energy $\tilde{\varepsilon}_{0,0}$ at site (0,0) is given by

$$\tilde{\varepsilon}_{0,0}=\varepsilon_{0,0}+\varepsilon_{0,0}^U+\varepsilon_{0,0}^R. \tag{33}$$

Further successively eliminating coefficients, $c_{n,0}$, with $n=0,-1,\cdots,-N_L$ in Eq. (32) gives

$$[E-\tilde{\varepsilon}_{-(N_L+1),0}]c_{-(N_L+1),0}+tc_{-(N_L+2),0}=0, \tag{34}$$

where

$$\tilde{\varepsilon}_{-(N_L+1),0}=\varepsilon_L+\cfrac{v_L^2}{E-\varepsilon_{-N_L,0}-\cfrac{t^2}{E-\varepsilon_{-(N_L-1),0}-\cfrac{t^2}{\ddots\cfrac{t^2}{E-\varepsilon_{-1,0}-\cfrac{t^2}{E-\tilde{\varepsilon}_{0,0}}}}}}. \tag{35}$$

Thus an equation [i.e., Eq. (34)] which contains only the expansion coefficients at the lattice sites $[-(N_L+1),0]$ and $[-(N_L+2),0]$ of the left-hand-side perfect lead has been obtained. The coefficients at lattice sites of the left-hand-side perfect lead can be generally written as

$$c_{n,0}=A^L e^{ik^L na}+B^L e^{-ik^L na}, \quad -\infty<n\leqslant-(N_L+1). \tag{36}$$

By combining this equation with Eq. (34), we readily obtain

$$B^L=-\frac{E-\tilde{\varepsilon}_{-(N_L+1),0}+te^{-ik^L a}}{E-\tilde{\varepsilon}_{-(N_L+1),0}+te^{ik^L a}}e^{-2ik^L(N_L+1)a}A^L. \tag{37}$$

Thus a simple relation for the amplitude of the reflected wave B^L, with the amplitude of the incoming wave A^L, is established. Using the boundary condition for the problem, $A^L=1$, and an equation similar to the formula shown in the first line of Eq. (14), we immediately obtain

$$\mathcal{R}_{11}=\left|\frac{E-\tilde{\varepsilon}_{-(N_L+1),0}+te^{-ik^L a}}{E-\tilde{\varepsilon}_{-(N_L+1),0}+te^{ik^L a}}\right|^2. \tag{38}$$

We emphasize again that this simple formula for the calculation of the reflectance $\mathcal{R}_{11}$ has been derived in a procedure which is very different from the procedure exploited in the first two ways, and is also different from the procedure used in the derivation for the transmissions $\mathcal{T}_{21}$ and $\mathcal{T}_{31}$.

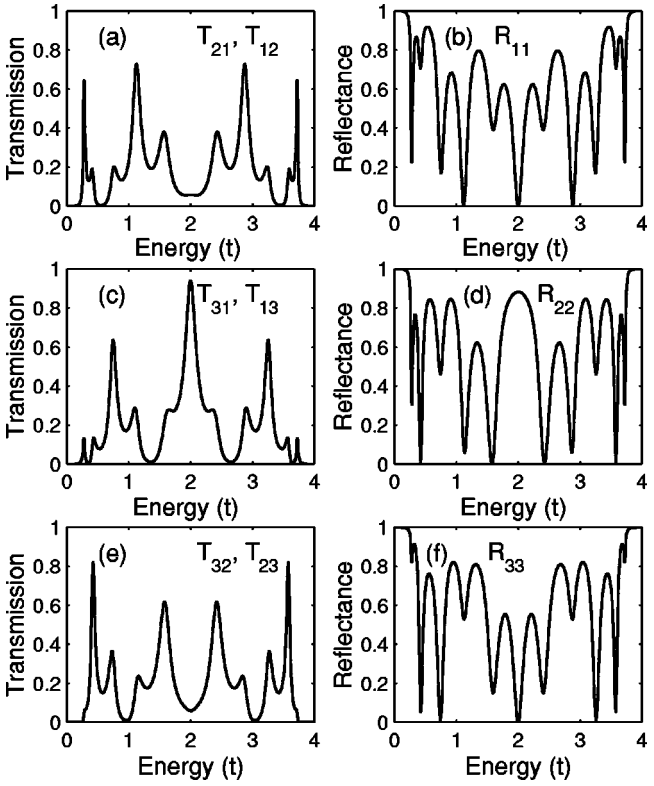

FIG. 4. Various transmission and reflection probabilities of the three-terminal, quantum-confined system as shown in Fig. 3, calculated as a function of the electron energy. The confined structure is modeled by a finite, T-shaped wire of 13 lattice sites. In the calculations, the structure parameters used are $N_L=5$, $N_R=4$, and $N_U=3$; the three coupling parameters are set at $v_L=0.5t$, $v_R=0.5t$, and $v_U=0.5t$; and all the on-site energies are assumed to have a value of $2t$. In the notations of T_{ij} and R_{ii} for the transmission and reflection probabilities, $i,j=1$ stands for the left-hand-side lead, $i,j=2$ for the right-hand-side lead, and $i,j=3$ for the upper-side lead.

So far, we have discussed only the formulations for the transmission probabilities $\mathcal{T}_{21}$ and $\mathcal{T}_{31}$ and the reflectance $\mathcal{R}_{11}$ of the three-terminal system. The formulations for the other scattering parameters (i.e., the transmission probabilities $\mathcal{T}_{12}$ and $\mathcal{T}_{32}$ and the reflectance $\mathcal{R}_{22}$, as well as the transmission probabilities $\mathcal{T}_{13}$ and $\mathcal{T}_{23}$ and the reflectance $\mathcal{R}_{33}$) of the three-terminal system can be carried out similarly. Finally, we would like to note that three of the six transmissions may also be obtained from the remaining three transmissions, if they are known, using the time-reversal symmetry $\mathcal{T}_{ij}=\mathcal{T}_{ji}$ in the absence of a magnetic field, and that the scattering parameters satisfy the equation $\mathcal{R}_{ii}+\Sigma_{j(\neq i)}\mathcal{T}_{ji}=1$ required by the current conservation.

As an example of application of the formalism presented in this subsection, we show in Fig. 4 the calculations for the transmission and reflection probabilities of a three-terminal, quantum-confined system as shown in Fig. 3 with the structure parameters of $N_L=5$, $N_R=4$, and $N_U=3$ and the coupling parameters of $v_L=v_R=v_U=0.5t$. Again, in the calculations, the on-site energies on all the lattice sites of the system have been assumed to have a value of $2t$. It is seen

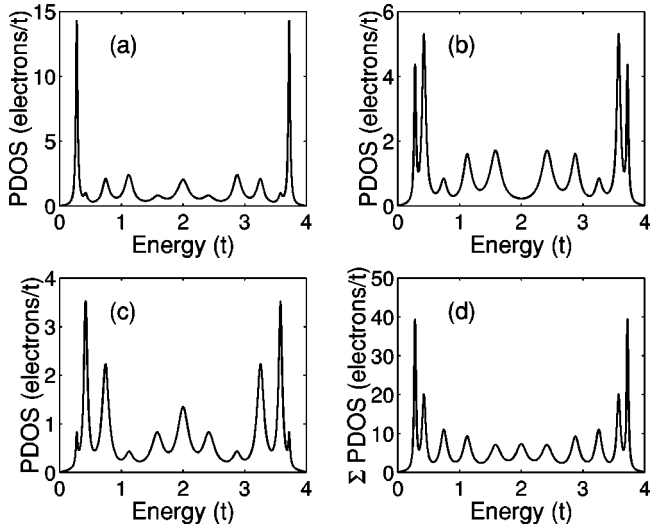

FIG. 5. Partial density of states (PDOS) calculated for the same three-terminal, quantum-confined system as in Fig. 3. (a) PDOS obtained by summing up the local densities of states on the five lattice sites of left-hand-side portion of the quantum-confined, T-shaped wire. (b) PDOS on the four lattice sites of right-hand-side portion of the quantum-confined, T-shaped wire. (c) PDOS on the three lattice sites of upper-side portion of the quantum-confined, T-shaped wire. (d) PDOS obtained by summing up the local densities of states on all the 13 lattice sites of the quantum-confined, T-shaped wire.

that the transmission and reflection probabilities show complicated spectra characterized by various sharp peaks or dips, except that the spectra are symmetric with respect to $E=2t$. By carefully examining the energy positions of all the peaks and dips, we can identify 11 resonant states of the system. This seems to be inconsistent with what one would expect for the system: the system has 13 localized states in the confined region, as the region is modeled by a finite T-shaped wire spanning 13 lattice sites. To understand the origin of this discrepancy, we have calculated the electronic structure of the system and have plotted, in Fig. 5(d), the partial density of states (PDOS) obtained by summing up the local densities of states (LDOS's) on all the 13 lattice sites of the confined region (see, e.g., Ref. 40 for the method of calculation). The calculation shows clearly that only 11 localized states are observable in the energy range of the conduction band of the perfect leads [see Fig. 5(d)]. Two other localized states are found to have energies staying outside of the conduction band of the perfect leads: one is at an energy below and the other one is at an energy above the conduction band. Thus these two states cannot be seen as resonances in the transmission and reflection probabilities of the system.

Figure 4 also shows that not all the 11 localized states at the energies within the conduction band of the perfect leads appear as resonances in every transmission or reflection probability of the system. This arises from the fact that the 11 states do not have same localizations in the confined region [see Figs. 5(a), 5(b), and 5(c)]. For example, by comparison of Figs. 4(b) and 5(a), we can find one-to-one correspondences between the sharp dips in the reflectance R_{11} and the peaks in the PDOS obtained by summing up the LDOS's

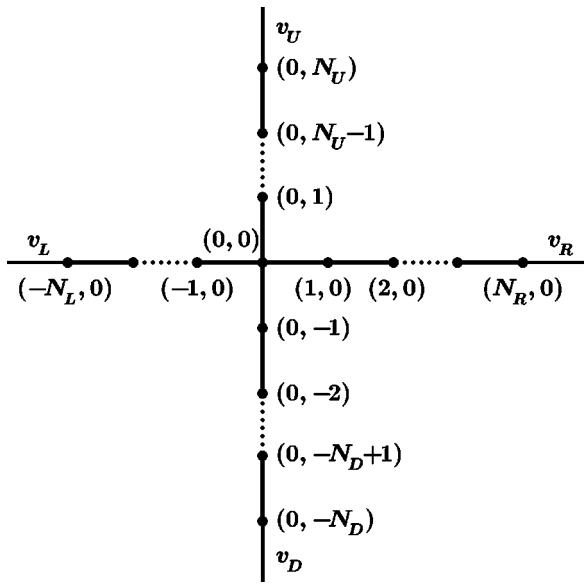

FIG. 6. Lattice model for the four-terminal, quantum-confined system. Here only the confined portion of the system with couplings to four leads described by parameters v_L, v_R, v_U, and v_D is given. The four leads are defined similarly as in Fig. 1.

on the lattice sites in the left portion of the confined, T-shaped region. Thus the electrons incident from the left-hand-side lead can be more easily coupled into the confined region and transmitted into the right-hand-side and/or upper-side lead, if there is a state, at the energy of the incident electrons, which has a large localization in the left portion of the confined region. A similar one-to-one correspondences can also be established between the sharp dips of reflectance R_{22} seen in Fig. 4(d) and the PDOS peaks seen in Fig. 5(b), as well as between the sharp dips of reflectance R_{33} seen in Fig. 4(f) and the PDOS peaks seen in Fig. 5(c). Thus similar explanations can be made for the dips seen in the reflection probabilities R_{22} and R_{33}. However, a peak in the transmission probability can be seen only when there exists a state, at the energy of the incident electrons, with large localizations in both the portion of the confined region, connecting to the lead where the electrons are incident from, and in the portion of the confined region, connecting to the lead where the electrons are transmitted into. For example, the transmission probability T_{21} from the left-hand-side lead to the right-hand-side lead does not show a peak at $E=2t$, although there is a state at this energy which has a large localization in the left portion of the confined region [see Fig. 5(a)]. This is because the state has a low PDOS on the right portion of the confined region [see Fig. 5(b)]. However, this state is strongly localized in the upper portion of the confined region [see Fig. 5(c)]. As a consequence, the transmission probability T_{31} from the left-hand-side lead to the upper lead shows a strong peak at $E=2t$ [see Fig. 4(c)].

C. Four-terminal system

The four-terminal system considered in the formulation is constructed, as shown in Fig. 6, by attaching four perfect leads to a cross-bar-shaped inhomogeneous region. The system can also be viewed as an extension of the three-terminal system (Fig. 3) discussed in the previous subsection. The parameters of coupling of the inhomogeneous region to the left-hand-, right-hand-, upper-, and down-side leads (labeled as leads 1 through 4) are denoted by v_L, v_R, v_U, and v_D, respectively (see Fig. 6). We again use a double-integer (i,j) scheme to label the lattice sites of the system and assign index (0,0) to the cross site. The inhomogeneous region now spans horizontal lattice sites $(-N_L,0)$, $(-N_L+1,0)$, $\ldots$,$(N_R-1,0)$, $(N_R,0)$ and vertical lattice sites $(0,-N_D)$, $(0,-N_D+1)$, $\ldots$,$(0,-1)$, and $(0,1)$, $\ldots$,$(0,N_U-1)$, $(0,N_U)$, while the four perfect leads span sites $(n,0)$ with $n\leqslant-(N_L+1)$, sites $(n,0)$ with $n\geqslant N_R+1$, sites $(0,n)$ with $n\geqslant N_U+1$, and sites $(0,n)$ with $n\leqslant-(N_D+1)$, respectively. The Hamiltonian of the system can be written as

$$H=H^{3T}+\sum_{n=-N_D}^{-1}\varepsilon_{0,n}\,a_{0,n}^{\dagger}a_{0,n}-\sum_{n=-N_D}^{-1}t(a_{0,n+1}^{\dagger}a_{0,n}+\text{H.c.})$$
$$+\sum_{n\leqslant-(N_D+1)}\varepsilon_D\,a_{0,n}^{\dagger}a_{0,n}-\sum_{n\leqslant-(N_D+2)}t(a_{0,n+1}^{\dagger}a_{0,n}+\text{H.c.})$$
$$-v_D(a_{0,-N_D}^{\dagger}a_{0,-N_D-1}+\text{H.c.}),\qquad(39)$$

where H^{3T} is the Hamiltonian of the three-terminal system discussed in Sec. II B, and is given by Eq. (15).

The scattering problem of the four-terminal system is again described by various transmission probabilities $\mathcal{T}_{ij}$ and reflection probabilities $\mathcal{R}_{ii}$, which are defined similarly as in Sec. II B for a three-terminal system. The derivations for these scattering parameters $\mathcal{T}_{ij}$ and $\mathcal{R}_{ii}$ follow rather similar procedures as in the case for the three-terminal system. Therefore, only a brief description of the formulation for the four-terminal system will be given.

We again consider the case of injection of electrons from the left, as an example. The eigensolutions of the four-terminal system can be written as

$$\psi^{\dagger}=\sum_{n=-\infty}^{\infty}c_{n,0}a_{n,0}^{\dagger}+\sum_{n=1}^{\infty}c_{0,n}a_{0,n}^{\dagger}+\sum_{n=-\infty}^{-1}c_{0,n}a_{0,n}^{\dagger}.\qquad(40)$$

The boundary conditions in the present case are

$$c_{n,0}=\begin{cases}A^Le^{ik^Lna}+B^Le^{-ik^Lna}, & -\infty<n\leqslant-(N_L+1)\\ A^Re^{ik^Rna}, & N_R+1\leqslant n<\infty,\end{cases}\qquad(41)$$

with $A^L=1$, and

$$c_{0,n}=\begin{cases}A^Ue^{ik^Una}, & (N_U+1)\leqslant n<\infty\\ B^De^{-ik^Dna}, & -\infty<n\leqslant-(N_R+1).\end{cases}\qquad(42)$$

We proceed first with our formulation for the transmission, $\mathcal{T}_{21}$, which is defined as the probability for electrons incident from the left to be transmitted to the right. To derive a formula for $\mathcal{T}_{21}$, we need to reduce the Schrödinger equation of the four-terminal system with the Hamiltonian given in Eq. (39) into the Schrödinger equation of an effective two-terminal system. This is done by inserting the eigensolution

expansion of Eq. (40), under the boundary conditions of Eqs. (41) and (42), into the Schrödinger equation of the original four-terminal system, and by eliminating all the coefficients, $c_{0,n}$, with $n \neq 0$. The result is

$$\begin{aligned}
&(E-\varepsilon_{-1,0})c_{-1,0}+tc_{-2,0}+tc_{0,0}=0,\\
&(E-\varepsilon_{1,0})c_{1,0}+tc_{0,0}+tc_{2,0}=0,\\
&[E-(\varepsilon_{0,0}+\varepsilon_{0,0}^{U}+\varepsilon_{0,0}^{D})]c_{0,0}+tc_{-1,0}+tc_{1,0}=0,\\
&\cdots\cdots\cdots\cdots,
\end{aligned} \tag{43}$$

with $\varepsilon_{0,0}^{U}$ given by Eq. (23) and $\varepsilon_{0,0}^{D}$ by

$$\varepsilon_{0,0}^{D}=\cfrac{t^2}{E-\varepsilon_{0,-1}-\cfrac{t^2}{E-\varepsilon_{0,-2}-\cfrac{t^2}{\ddots\;\cfrac{t^2}{E-\varepsilon_{0,-N_D}-\Sigma^{D}(E)}}}}, \tag{44}$$

where

$$\Sigma^{D}(E)=v_D^2 G^{D}(E) \tag{45}$$

is the self-energy due to the presence of the down-side perfect lead, and

$$G^{D}(E)=[E-\varepsilon_D-t^2 G^{D}(E)]^{-1} \tag{46}$$

is the Green's function at the first site of the down-side lead. Now, starting from the equation system shown in Eq. (43), it becomes straightforward to calculate the transmission of the four-terminal system, $\mathcal{T}_{21}$, by applying the formalism developed in Sec. II A for a two-terminal system [also see Sec. II B and, in particular, Eq. (26)].

The transmissions of the four-terminal system, $\mathcal{T}_{31}$ and $\mathcal{T}_{41}$, can be calculated in similar procedures. However, the following changes need to be made. When the transmission $\mathcal{T}_{31}$ is calculated, $\varepsilon_{0,0}^{U}$ in Eq. (43) needs to be replaced by $\varepsilon_{0,0}^{R}$, which is given by Eq. (27). While when the transmission $\mathcal{T}_{41}$ is calculated, $\varepsilon_{0,0}^{D}$ (instead of $\varepsilon_{0,0}^{U}$) in Eq. (43) needs to be replaced by $\varepsilon_{0,0}^{R}$.

Similar to the calculation for a three-terminal system, the reflectance of the four-terminal system, $\mathcal{R}_{11}$, can be calculated with various equivalent methods. It can be calculated at the same time the transmission $\mathcal{T}_{21}$ is calculated, by applying the formalism developed in Sec. II A for a two-terminal system. It can also be obtained at the time $\mathcal{T}_{31}$ or $\mathcal{T}_{41}$ is calculated. In addition, the reflectance of the four-terminal system, $\mathcal{R}_{11}$, can straightforwardly be calculated from Eq. (38) with $\tilde{\varepsilon}_{-(N_L+1),0}$ given by Eq. (35) and $\tilde{\varepsilon}_{0,0}$ in Eq. (35) by

$$\tilde{\varepsilon}_{0,0}=\varepsilon_{0,0}+\varepsilon_{0,0}^{U}+\varepsilon_{0,0}^{D}+\varepsilon_{0,0}^{R} \tag{47}$$

instead of Eq. (33).

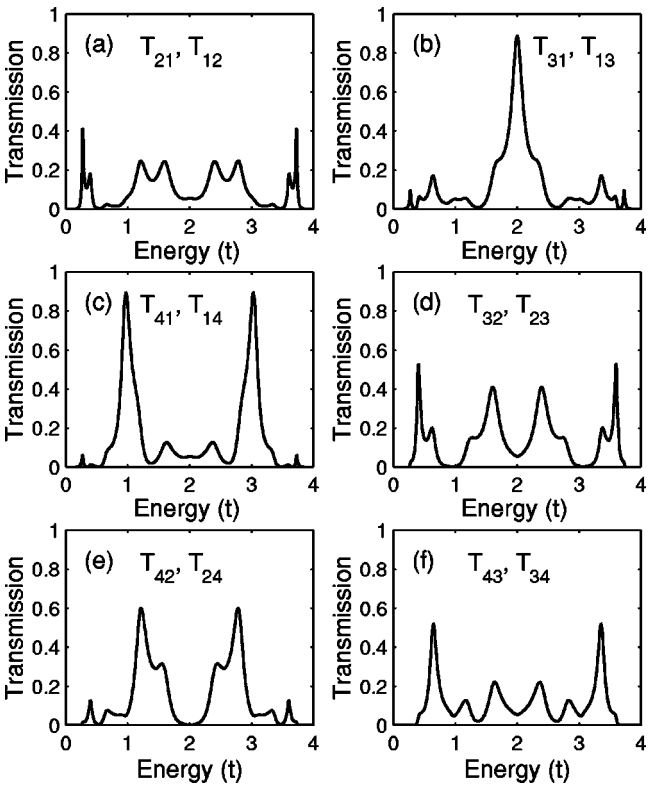

FIG. 7. Various transmission probabilities of a four-terminal, quantum-confined system as shown in Fig. 6, calculated as a function of the electron energy. Here the confined structure is modeled by a finite, cross-bar-shaped wire. In the calculations, the structure parameters used are $N_L=5$, $N_R=4$, $N_U=3$, and $N_D=2$; the four coupling parameters are set at $v_L=0.5t$, $v_R=0.5t$, $v_U=0.5t$, and $v_D=0.5t$; and all the on-site energies are assumed to have a value of $2t$. In the notations of T_{ij}, $i,j=1$ stands for the left-hand-side lead, $i,j=2$ for the right-hand-side lead, $i,j=3$ for the upper-side lead, and $i,j=4$ for the down-side lead.

Other scattering parameters of the four-terminal system are the transmission probabilities, $\mathcal{T}_{ij}$ with $i=1,2,3,4$, $j=2,3,4$, and $i \neq j$, and the reflection probabilities, $\mathcal{R}_{ii}$ with $i=2,3,4$. These parameters can be obtained in the same way as described above for the calculations of the transmissions $\mathcal{T}_{21}$, $\mathcal{T}_{31}$, and $\mathcal{T}_{41}$ and the reflectance $\mathcal{R}_{11}$. Furthermore, after a sufficient number of scattering parameters of the four-terminal system are obtained, the remaining scattering parameters can also be obtained using the time-reversal symmetry, $\mathcal{T}_{ij}=\mathcal{T}_{ji}$, in the case of the absence of magnetic field, and the current conservation, $\mathcal{R}_{ii}+\Sigma_{j(\neq i)}\mathcal{T}_{ji}=1$.

Again as an example of application of the present formalism, we have calculated various transmission and reflection probabilities of a four-terminal system, as shown in Fig. 6 with the structure parameters $N_L=5$, $N_R=4$, $N_U=3$, and $N_D=2$, the coupling parameters $v_L=v_R=v_U=v_D=0.5t$, and the on-site energies $2t$ on all the lattice sites of the system. The results of the calculation are presented in Figs. 7 and 8. As in the calculations for the three-terminal system, the transmission and reflection probabilities of the four-terminal system show various sharp peaks or dips. Overall, 13 resonant states can be identified from the spectra of the

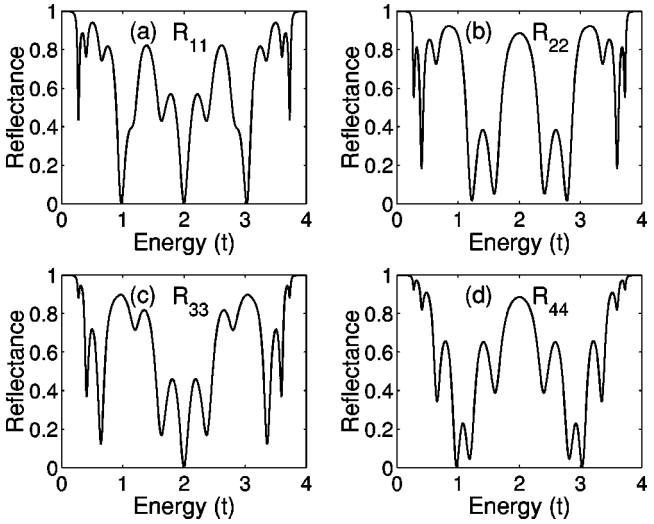

FIG. 8. Various reflection probabilities of the same four-terminal, quantum-confined system as in Fig. 7, as a function of the electron energy.

transmission and reflection probabilities. This result is consistent with the calculation for the PDOS, obtained by summing up the LDOS's on all 15 lattice sites of the confined region, shown in Fig. 9(e), where 13 PDOS peaks corresponding to 13 localized states of the system are clearly seen in the energy range of the conduction band of the perfect leads. Here we note that the confined, cross-bar-shaped system considered in this subsection has 15 localized states. However, as in the three-terminal, T-shaped system studied in Sec. II B, two of these 15 states, which do not appear in the calculated PDOS shown in Fig. 9(e), are located at energies below and above the energy band of the perfect leads, respectively. Thus these two states cannot be seen as resonances in the transmission and reflection probabilities of the four-terminal system.

Figures 9(a)–9(d) show that the 13 localized states of the system at energies within the conduction band of the perfect leads are very different in their properties of localization. For example, the state at $E=2t$ is largely localized in the left-hand-side and upper-side portions of the quantum-confined, cross-bar structure, and contains little contributions from the orbitals on the lattice sites in the right-hand-side and down-side portions of the quantum-confined, cross-bar structure. However, the states at $E=0.27t$ and $3.73t$ are seen to be strongly localized on the left-hand-side portion of the quantum-confined, cross-bar structure.

The reflectance spectra of the four-terminal system, shown in Fig. 8, are seen to be very different from each other. However, all the dips in the reflectance spectra can be found to correspond to a peak in the PDOS's shown in Figs. 9(a)–9(d). These one-to-one correspondences between the dips in the reflection probabilities and the peaks in the PDOS's of the four-terminal system can be explained in the same way as in Sec. II B for the three-terminal system. The various transmission peaks seen in Fig. 7 can also be explained, as in the previous subsection, based on the localization properties of the 13 localized states of the four-terminal system shown in Figs. 9(a)–9(d).

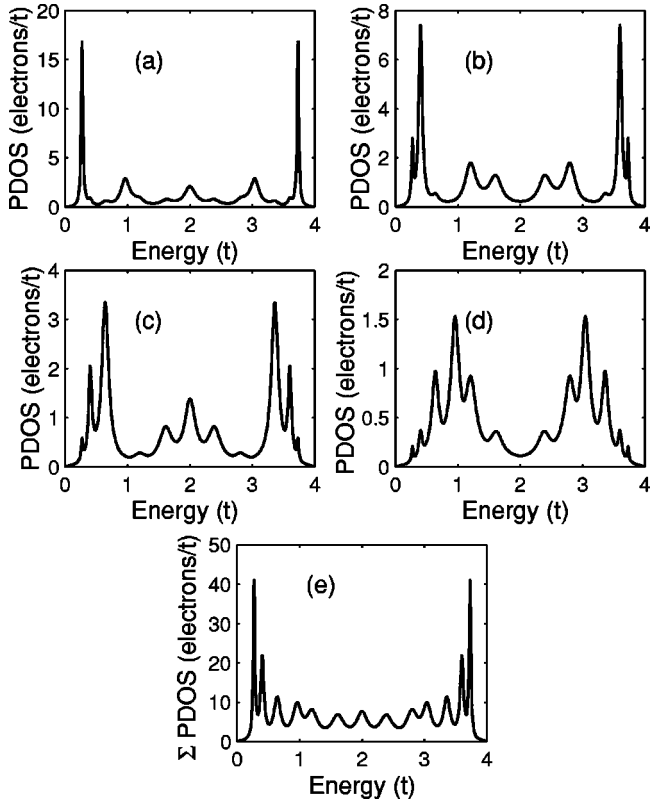

FIG. 9. Partial density of states (PDOS) calculated for the same four-terminal, quantum-confined system as in Figs. 7 and 8. (a) PDOS obtained by summing up the local densities of states on the five lattice sites of left-hand-side portion of the quantum-confined, cross-bar-shaped wire. (b) PDOS on the four lattice sites of right-hand-side portion of the quantum-confined, cross-bar-shaped wire. (c) PDOS on the three lattice sites of upper-side portion of the quantum-confined, cross-bar-shaped wire. (d) PDOS on the two lattice sites of down-side portion of the quantum-confined, cross-bar-shaped wire. (e) PDOS obtained by summing up the local densities of states on all 15 lattice sites of the quantum-confined, cross-bar-shaped wire.

III. SUMMARY AND CONCLUSIONS

In this paper, we have presented a formalism for calculations of various properties of electron transport in multiterminal quantum systems. The systems were described by lattice models. By exploiting real-space Green's functions, we have derived, for calculations of the transmission and reflection probabilities of each multiterminal system, various effective two-terminal systems. Thus the properties of electron transport can be studied based on a standard two-terminal method, such as the transfer-matrix or Green's function method.

The formalism has been applied to a three-terminal system, containing a quantum-confined, T-shaped structure, and a four-terminal system, containing a quantum-confined, cross-bar structure. The calculations reveal that the two multiterminal systems show complex transmission and reflection spectra. This is in strong contrast to the calculation for a two-terminal double-barrier structure in which the transmission and reflection probabilities show regular resonant struc-

tures. To understand the results of the calculations for the multiterminal systems, we have calculated partial densities of states on the lattice sites of the confined regions. We have found that the complexity of the transmission and reflection spectra of the multiterminal systems arises from the fact that the confined states in the systems are localized in different parts of the confined regions and can contribute very differently to different transmission and reflection probabilities of the systems.

Our formalism can easily be generalized to treat various other multiterminal and/or complex systems. It can also be generalized to include electron-electron interactions and to treat electron transport in multiterminal systems under finite bias (i.e., in the nonlinear response regime). Some preliminary results of such generalizations have been reported,[38,50,51] and the detailed calculations will be published elsewhere.

ACKNOWLEDGMENTS

This work, which was performed within the Nanometer Consortium at Lund University, was supported by the Swedish Foundation for Strategic Research (SSF) and the Swedish Research Council (VR).

*Electronic address: Hongqi.Xu@ftf.lth.se

[1] R. Landauer, IBM J. Res. Dev. **1**, 223 (1957).
[2] E.N. Economou and C.M. Soukoulis, Phys. Rev. Lett. **46**, 618 (1981).
[3] D.S. Fisher and P.A. Lee, Phys. Rev. B **23**, 6851 (1981).
[4] M. Büttiker, Phys. Rev. Lett. **57**, 1761 (1986).
[5] J. Kucera and P. Streda, J. Phys. C **21**, 4357 (1988).
[6] G. Kirczenow, Phys. Rev. B **39**, 10452 (1989).
[7] S.E. Ulloa, E. Castañ̃o, and G. Kirczenow, Phys. Rev. B **41**, 12350 (1990).
[8] J.A. Brum, Phys. Rev. B **43**, 12082 (1991).
[9] H. Tamura and T. Ando, Phys. Rev. B **44**, 1792 (1991).
[10] H. Wu, D.W.L. Sprung, J. Martorell, and S. Klarsfeld, Phys. Rev. B **44**, 6351 (1991).
[11] H. Wu and D.W.L. Sprung, Phys. Rev. B **47**, 1500 (1993).
[12] H.Q. Xu, Zhen-Li Ji, and K.-F. Berggren, Superlattices Microstruct. **12**, 237 (1992).
[13] H.Q. Xu, Phys. Rev. B **47**, 9537 (1993).
[14] H.Q. Xu, Phys. Rev. B **50**, 8469 (1994).
[15] H.Q. Xu, Phys. Rev. B **52**, 5803 (1995).
[16] Z.-L. Ji, Phys. Rev. B **50**, 4658 (1994).
[17] D.J. Thouless and S. Kirkpatrick, J. Phys. C **14**, 235 (1981).
[18] P.A. Lee and D.S. Fisher, Phys. Rev. Lett. **47**, 882 (1981).
[19] L. Schweizer, B. Kramer, and A. MacKinnon, J. Phys. C **17**, 4111 (1984).
[20] L. Schweizer, B. Kramer, and A. MacKinnon, Z. Phys. B: Condens. Matter **59**, 379 (1985).
[21] A. MacKinnon, Z. Phys. B: Condens. Matter **59**, 385 (1985).
[22] T. Ando, Phys. Rev. B **44**, 8017 (1991).
[23] K. Shepard, Phys. Rev. B **43**, 11623 (1991).
[24] M. Büttiker, Y. Imry, and M.Ya. Azbel, Phys. Rev. A **30**, 1982 (1984).
[25] D.G. Ravenhall, H.W. Wyld, and R.L. Schult, Phys. Rev. Lett. **62**, 1780 (1989).
[26] H.U. Baranger and A.D. Stone, Phys. Rev. Lett. **63**, 414 (1989).
[27] R.L. Schult, H.W. Wyld, and D.G. Ravenhall, Phys. Rev. B **41**, 12760 (1990).
[28] J.B. Xia, Phys. Rev. B **45**, 3593 (1992).
[29] J. Wang, Y.J. Wang, and H. Guo, Phys. Rev. B **46**, 2420 (1992).
[30] O. Vanbésien and D. Lippens, Appl. Phys. Lett. **65**, 2439 (1994).
[31] M. Shin, S. Lee, K.W. Park, and E.-H. Lee, Phys. Rev. B **50**, 11192 (1994).
[32] T. Itoh, Phys. Rev. B **52**, 1508 (1995).
[33] W.D. Sheng and H.Q. Xu, J. Appl. Phys. **84**, 2146 (1998).
[34] P.A. Mello, Phys. Rev. B **47**, 16358 (1993).
[35] D. Takai and K. Ohta, Phys. Rev. B **48**, 1537 (1993).
[36] H.Q. Xu and W.D. Sheng, Phys. Rev. B **57**, 11903 (1998).
[37] C.M. Ryu and S.Y. Cho, Phys. Rev. B **58**, 3572 (1998).
[38] H.Q. Xu and B.-Y. Gu, J. Phys.: Condens. Matter **13**, 3599 (2001).
[39] R. Haydock, V. Heine, and M.J. Kelly, J. Phys. C **5**, 2845 (1972).
[40] H.Q. Xu and U. Lindefelt, Phys. Rev. B **41**, 5979 (1990).
[41] Th. Martin and R. Landauer, Phys. Rev. B **45**, 1742 (1992).
[42] H.-W. Lee and C.S. Kim, Phys. Rev. B **63**, 075306 (2001).
[43] H.-W. Lee, Phys. Rev. Lett. **82**, 2358 (1999).
[44] T. Taniguchi and M. Büttiker, Phys. Rev. B **60**, 13814 (1999).
[45] A. Oguri, Phys. Rev. B **59**, 12240 (1999).
[46] A. Oguri, Phys. Rev. B **63**, 115305 (2001).
[47] O. Entin-Wohlman, A. Aharony, and Y. Levinson, Phys. Rev. B **64**, 085332 (2001).
[48] See, for example, S. Datta, in *Electronic Transport in Mesoscopic Systems* (Cambridge University Press, Cambridge, 1995).
[49] See, for example, Y. Liu and R. Riklund, Phys. Rev. B **35**, 6034 (1987).
[50] H.Q. Xu, Ann. Phys. (Leipzig) **8**, SI-289 (1999).
[51] S.D. Wang, Z.Z. Sun, N. Cue, H.Q. Xu, and X.R. Wang, Phys. Rev. B **65**, 125307 (2002).